Effect of surface nanostructure on tensile and low cycle fatigue behavior of Al 2014 alloy

To cite this article: K Chattopadhyay *et al* 2014 *IOP Conf. Ser.: Mater. Sci. Eng.* **63** 012017

View the article online for updates and enhancements.

Related content

- Fatigue properties of a biomedical 316L steel processed by surface mechanical attrition
  Z Sun, M Chemkhi, P Kanoute et al.

- From conventional to severe shot peening to generate nanostructured surface layer: A numerical study
  S M Hassani-Gangaraj, A Moridi and M Guagliano

- Effect of stress relieving treatment on low cycle fatigue behavior of USSP treated 7075 aluminium alloy
  Vaibhav Pandey, K. Chattopadhyay, N. C. Santhi Srinivas et al.

Recent citations

- Effect of Ultrasonic Shot Peening on Surface Microstructure and Fatigue Behavior of Structural Alloys
  Vakil Singh *et al*

Effect of surface nanostructure on tensile and low cycle fatigue behavior of Al 2014 alloy

K Chattopadhyay*, V Pandey, N C S Srinivas, V Singh

Department of Metallurgical Engineering, Indian Institute of Technology
(Banaras Hindu University), 221005 Varanasi, India.
*E-mail address: kausik.met@iitbhu.ac.in

Abstract. Aluminium alloy 2014 is an important age hardening alloy for aerospace industries. Effect of ultrasonic shot peening (USSP) in peak aged condition of this alloy was studied on its surface microstructure, tensile properties and low cycle fatigue behavior. The structure of the USSP treated specimens, close to surface was characterized by X-ray diffraction and transmission electron microscopy. The top surface region was found to contain nanosize grains of ~30 nm. Both yield as well as tensile strength was found to increase progressively with increasing duration of shot peening for 10, 15 and 20 minutes. LCF behavior was studied following ultrasonic shot peening for 10 minutes, at three total strain amplitudes ($\Delta\varepsilon_t/2$) of ±0.4%, ±0.5% and ±0.6%.

Keywords: 2014 aluminium alloy, ultrasonic shot peening, surface nanocrystallization, low cycle fatigue.

1. Introduction

Aluminium alloy 2014 is an important age hardening alloy and is extensively used in aircraft industries because of its high specific strength. However, there is much scope of improvement in its fatigue resistance.

It is well established that fatigue, fretting fatigue, wear and corrosion are highly sensitive to structure and properties of surface of the components and in most cases failures originate from surface. Optimization of structure and properties of surface may effectively enhance service life of structural components. Introduction of compressive residual stress and presence of nanostructure at surface is known to increase fatigue life of structural metallic components. Last few decades have seen considerable scientific interest in ultrafine-grained materials, especially nanocrystalline (NC), with size up to 100 nm [1-6]. Nanostructuring at the surface is known to enhance fatigue resistance without any modification in the chemical compositions and shape of the components [7].

Ultrafine-grained structures have been achieved by severe plastic deformation (SPD) through imposition of intense plastic strains. The microstructure resulting from severe plastic deformation is substantially reduced in grain size, and associated with high internal stresses along with high-energy non equilibrium boundaries [8].The requisite high plastic strain of the order of several hundreds of percent can be produced by various available techniques, such as equal-channel angular pressing (ECAP) [9-11], high-pressure torsion [12] , sliding wear [13,14], ball milling [15,16], shot blasting [17,18], ultrasonic shot peening [19-24] and air blast shot peening [25,26]. Ultrasonic shot peening (USSP) is considered to be an effective means of surface grain refinement through severe plastic deformation of surface to nanosize. In USSP, there is bombardment of surface of work piece with metallic projectile balls, to create a layer of severe plastic deformation at the surface. During the process of USSP, ultrafine grain structures are produced due to intense strain and high strain rates in the surface region. These intense strains give rise to strain gradient in the surface region, varying from a maximum at the top surface to zero at some depth in the matrix [12]. Higher intensity shot peening increases the depth of compressed region by virtue of increasing the duration of shot bombardment, peening with larger balls or at higher amplitude, or both. Increase in shot peening intensity, however, increases roughness of the surface and the level of cold work at the surface, both of which are known to reduce fatigue performance [26].

The recent work of *Abood et al.* [27] on AA 2024-T4 has revealed that its tensile and yield strength increased due to shot peening and attained highest value at 15 minutes of shot peening. Longer peening caused decline in strength. LCF tests showed that increase in shot peening duration led to reduction in transition fatigue life (N_T), till 15 minutes of peening. *Curtis et al.* [28] made two propositions; resistance to development of crack tip plasticity increased by work hardening of the peened layer and resistance to crack opening or closure of crack increased by the compressive residual stress. *Luong et al.* [29] used two techniques, namely shot peening and laser peening on 7050-T7451 and reported that out of the two techniques, laser peening induced a layer of compressive residual stress more than three times deeper than that from shot peening , though both the treatments were found to increase the fatigue performance significantly. However, limited research is available on the effect of ultrasonic shot peening on low cycle fatigue behavior of 2014 aluminium alloy.

The objective of the present investigation was to study the effect of ultrasonic shot peening (USSP) on microstructure in surface region, tensile properties and LCF behavior of the precipitation hardened 2014 aluminium alloy. The material was tested for the above characteristics both in peak aged (175°C for 8 hrs) as well as peak aged and shot peened condition.

2. Materials and Methods

The nominal chemical composition the 2014 aluminium alloy used in the present investigation was determined by spark emission spectrometer and is presented in Table 1. The material was solution treated at 500°C for 2 hrs, quenched in water and subjected to peak ageing at 175°C for 8 hrs and cooled in air.

Table 1 Chemical Composition of the aluminium alloy 2014 (wt%)

	Cu	Mg	Mn	Si	Fe	Cr	Zn	Al
Wt%	4.38	0.45	0.51	0.54	0.29	0.004	0.03	Bal.

Disks of 5 mm thickness and 23 mm diameter were used for USSP by SONATS Stress Voyager in order to characterize the microstructural modification using transmission electron microscopy. Ultrasonic shot-peening treatment of the alloy 2014 was performed with steel balls of 3mm diameter at amplitude of 80 μm for different lengths of time (Table 2).

Table 2 Effect of USSP treatments on Microhardness and Depth of modified layer

S. No.	Ball size (mm)	Amplitude (μm)	Peening time (min)	Microhardness at surface (Hv)	Depth of modified layer (μm)
1			10	258	962
2	3	80	15	261	686

Optical metallography of the specimens in solutionized and peak aged condition was carried out following mechanical polishing and etching with a solution of 95 ml H_2O, 2.5 ml HNO_3, 1.5 ml HCl and 1.0 ml HF at room temperature. Microstructure was examined using image analyzer. Microhardness was measured using Shimadzu micro hardness tester at applied load of 100g and dwell time of 5 seconds. TEM foils of the USSP treated surface layer were prepared by cutting a thin slice near the shot peened region and subsequently electro chemical polishing using an electrolyte of 20% nitric acid in methanol at -30°C at applied voltage of 22V. Transmission electron microscopic (TEM) examinations were carried out on a TECNAI 20 G^2 transmission electron microscope operating at 200 kV. A Rigaku X-ray diffractometer with Cu Kα radiation was used to determine phase constitution and mean grain size at room temperature in the shot peened condition. Crystallographic structure of the USSP treated samples was characterized by XRD in the 2θ range from 20° to 80°. The grain size was calculated from line broadening of Bragg diffraction peaks using Scherrer and Wilson Method [30].

Tensile properties were determined using a 100 kN screw-driven Instron™ (Model 4206) universal testing machine, at a strain rate of 5×10^{-3} s^{-1}, at room temperature. All the tensile test specimens were prepared with gage length and diameter of 15.4 mm and 4.5 mm respectively.

LCF tests were conducted on a servo hydraulic MTS™ of 50 kN (Model 810) under total strain control mode with triangular wave form and fully reversed axial loading (R = -1), at different strain amplitudes. Cylindrical LCF test specimens with threaded ends of 30 mm length and 12 mm diameter, gage section of 15 mm length and 5.5 mm diameter and shoulder radii of 25 mm were machined from the heat-treated blanks.

3. Results and Discussion

3.1 Microstructure

Figs. 1 (a) and (b) show optical microstructures of the alloy in solution treated and peak aged condition (175°C for 8 hours) respectively.
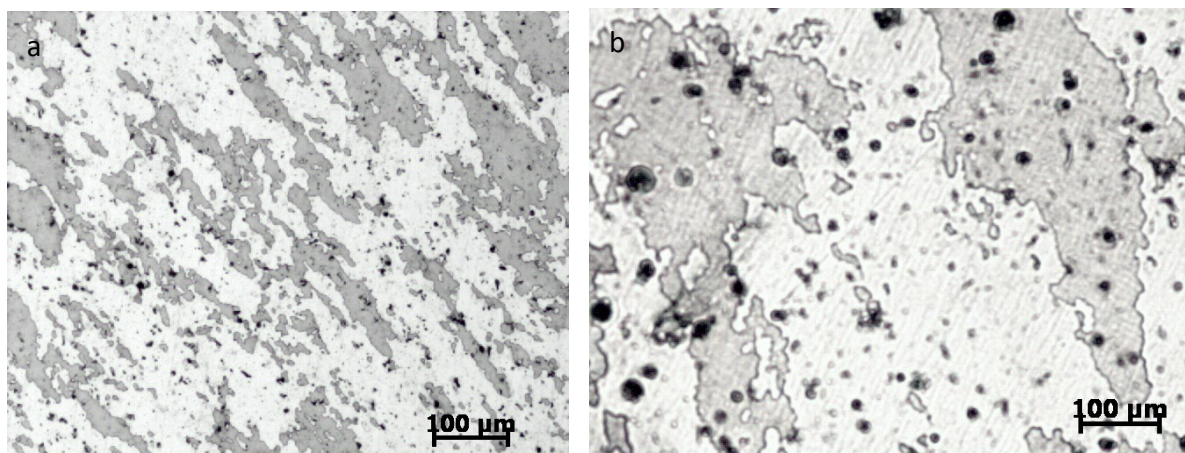

Figure 1 Optical micrographs of the 2014 aluminium alloy (a) solutionized condition (b) peak aged condition

Two different types of intermetallic particles, $CuAl_2$ with white outlined structure and dark complex compound of $Al_{12}(Fe,Mn)_3Si$ may be seen. Dispersoids and coarse precipitates are known to cause highly heterogeneous deformation and consequent damage to fatigue resistance [31, 32]. It may be seen that in the solution treated condition the amount of dispersoids was less as compared to that in the peak aged condition. The average grain size of the solutionized and peak aged samples was found to be 76 µm and 92 µm respectively.

3.2 Effect of Ultrasonic Shot Peening:

3.2.1 Microstructure

Fig. 2 shows X-ray diffraction (XRD) profiles of solutionized samples subjected to different durations of shot peening.
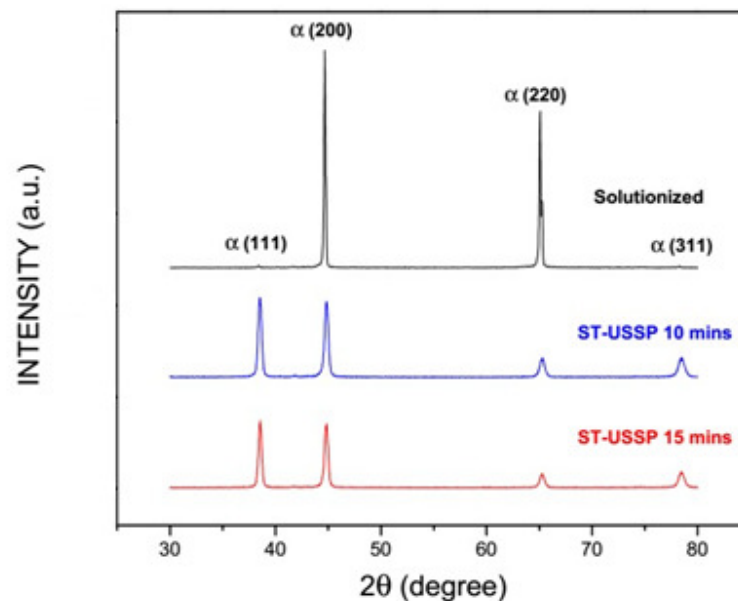

Figure 2 XRD profiles of 2014 aluminium alloy in solutionized and peak aged condition and shot peened for different durations.

It is obvious from XRD profile that there was no phase transformation in surface layer of the alloy 2014 from USSP treatment. However, the Bragg diffraction peaks after USSP treatment became broader than those of the original sample, suggesting grain refinement and/or an increase in the atomic level lattice strain [33, 34]. With increase in USSP time the intensity of peaks decreased revealing slight change in average grain size in the top surface layer. It may be seen that as the duration of shot peening time increased Bragg peaks broadened and the grain size was reduced.

Fig. 3 show TEM micrographs of surface region of the samples shot peened for 10 mins. It can be seen that nanocrystalline grains were formed after shot peening treatment and were mostly equiaxed with random crystallographic orientations same as observed by *Blonde et.al* on Cu [35]. The average grain size measured from bright field micrographs was found to be ~30 nm for the samples treated for 10 min whereas for un-shot peened specimen it is in the range of 10-600 nm [36] .
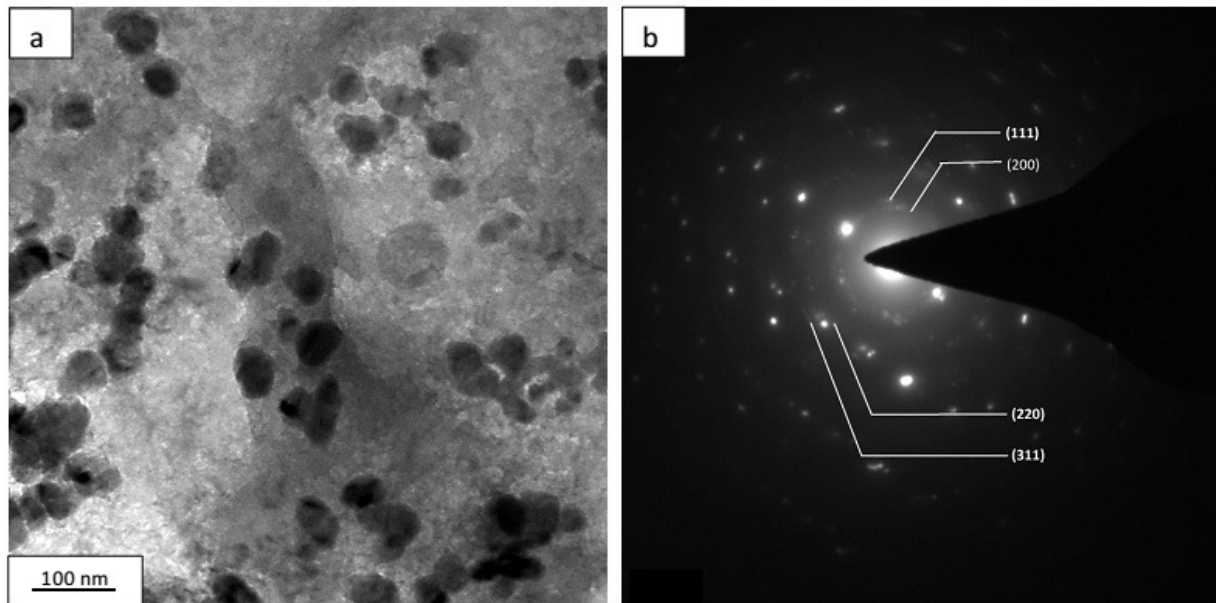
Figure 3 Bright Field TEM micrograph and corresponding SAD pattern: (a) 10 minutes of USSP treatment (b) Corresponding SAD pattern

The SAD pattern showed formation of discontinuous ring pattern and confirmed drastic grain refinement and formation of nanosized grains. The SAD pattern showed partially developed circle with well-defined diffraction spots, indicating microbands consisting of low angle misorientations [12]. The subsequent shot peening results into annihilation or rearrangement of a large number of dislocations, to form small angle grain boundaries separating individual grains. Formation of nanocrystalline structure in the surface layer due to ultrasonic shot peening treatment had its familiarity with the process of nanostructuring by severe plastic deformation of metals and alloys, involving generation of repeated multidirectional mechanical loads at high speeds onto the surface of the material. Further, USSP resulted into formation of crystallites with completely random orientation.

3.2.2 Microhardness

The variation of microhardness in transverse section of the shot peened specimen, from surface towards interior, is shown in Fig. 4. Microhardness of the top surface increased with increase in shotpeening time and the effectiveness of shot peening also increased to larger depth from the surface and it gradually decreased with increase in distance from the surface towards interior.
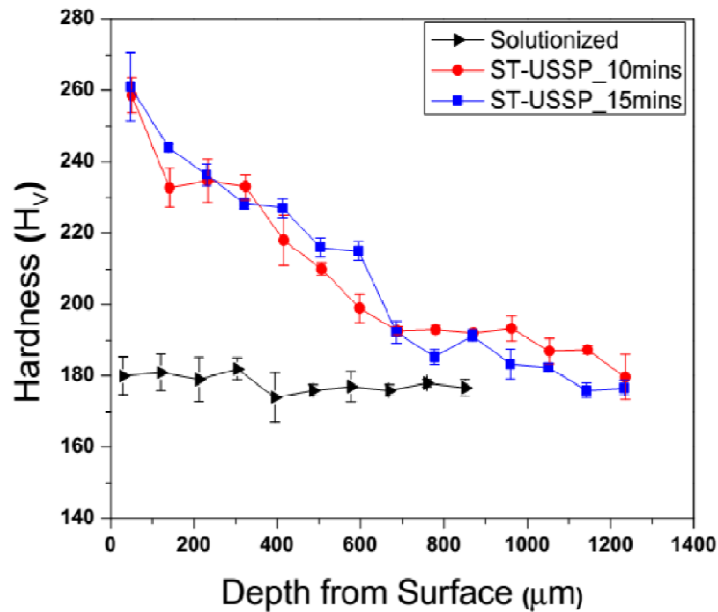
Figure 4 Variation of microhardness with depth from the surface in longitudinal section of USSP treated sample of the solutionized 2014 aluminium alloy, for different durations of peening.

The hardness of the unshotpeened sample was 181 VHN and that of shotpeened sample was reduced significantly from top surface to the depth of about 500 μm. It is conventional that effect of USSP treatment on the hardness profile was limited to a depth of ~500 μm. Increase in microhardness at surface was from refinement of microstructure resulting from shot peening by hard balls and formation of porosity free highly dense nanocrystallized surface layer. Thus, the material after USSP treatment unveiled better mechanical properties. The increase in grain size with increase in depth from the peened surface is in line with earlier observations [37, 38].

3.2.3 Tensile properties

It is evident from Fig.5 that yield strength (σ_y) and tensile strength (σ_u) increased with duration of shot peening upto 15 minutes and declined with further increase in peening time. The yield strength was 469 MPa with ~13% increment. Tensile strength increased to 531 MPa which was ~9% higher than to that of the un-shotpeened specimen. Ductility decreased from 17% to 11% with increase in time of shot peening upto 20 minutes.
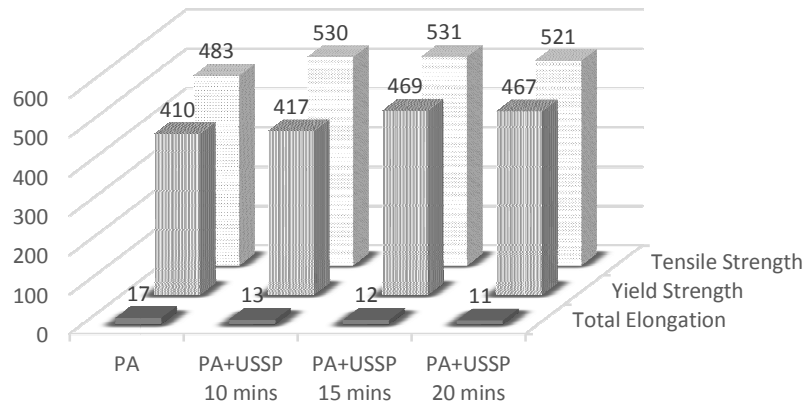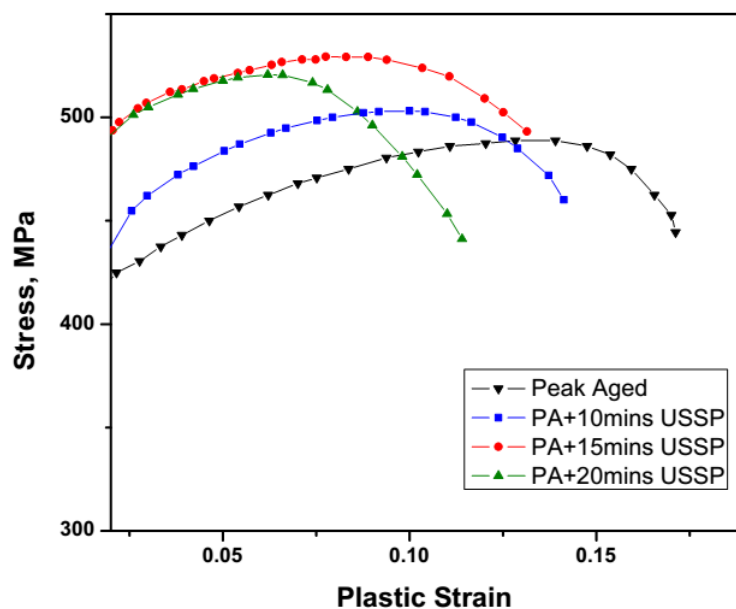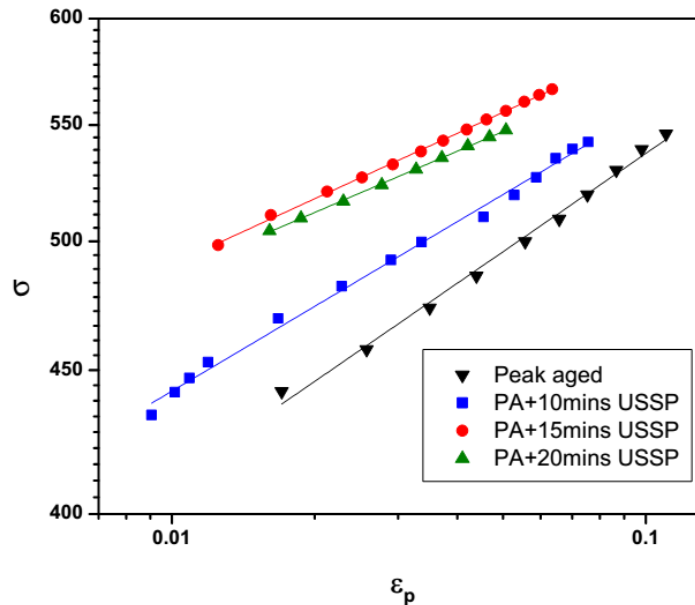
Figure 5 Variation of yield & tensile strength and total elongation with peening time.

The engineering stress-plastic strain curves and the log-log plots of the true stress *vs* true plastic strain are depicted in Figs.6 (a) and (b) respectively.

(a)

(b)

Figure 6 (a) Engineering stress-engineering plastic strain curves (b) True stress-plastic strain plots on log log scale for different conditions of the alloy 2014.

The best combination of ultimate tensile strength and yield strength with adequate ductility was exhibited by the specimen shot peened for 15 mins. The degree of work hardening was highest in the peak aged specimen followed by USSP treated samples for 10 mins, 20 mins and 15 mins respectively. Tensile data of the as received and different shot peened specimens was analyzed using Hollomon relationship, $\sigma = K\varepsilon^{n}_{p}$, [39] where K and n are the strength coefficient and strain hardening exponent respectively. Work-Hardening parameters for the different conditions are listed in Table 3.

Table 3 Work-hardening parameters of the 2014 Aluminium alloy in different conditions

S. No.	Designation	K (MPa)	n
1	PA	702	0.11
2	PA+USSP 10mins	635	0.06
3	PA+USSP 15mins	655	0.05
4	PA+USSP 20mins	631	0.04

The n value of the shotpeened sample was found to be much smaller than that of the unshotpeened one. The surface roughness of un-shot peened tensile specimen was measured and found to be 0.192 μm whereas value of surface roughness for the USSP sample treated for

10 mins, 15 mins and 20 mins was 2.463 µm, 2.895 µm and 3.455 µm respectively. *Roland et al.* [34] also observed enhancement in tensile properties of 316L stainless steel from SMAT processing. As reported earlier by Xing et al. [40] increase in strength could be due to strain-induced nanostructured layer which enhanced strength and rigidity of the surface so that the initiation of cracks and defects was reduced, in addition formation of slip bands was inhibited due to nanostructured surface. The decrement in values of σ_u and σ_y of the samples, shotpeened for more than 15 minutes, may be due to increase in surface roughness which was more effective than the compressive residual stresses. This observation is similar to that made by *Abood et al.* [27] in aluminium alloy 2024-T4 and signifies the role of surface roughness on loss of properties. The value of strain hardening exponent (n) also decreased with increase in peening time indicating loss of work hardening due to very low dislocation storage efficiency inside tiny grains of the refined microstructure [41].

3.2.4 Low Cycle Fatigue behavior

Cyclic stress response curves of the peak aged and peak aged ultrasonic shot peened specimen for 10 minutes are shown in Fig. 7 at different total strain amplitudes.
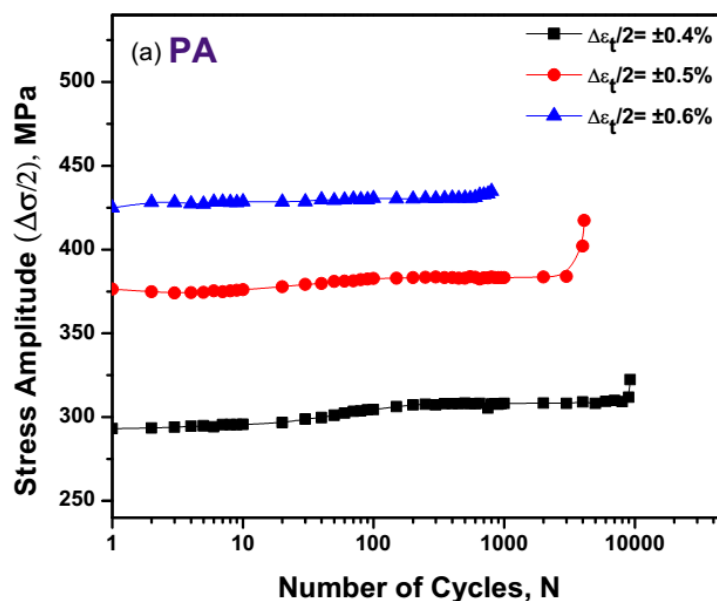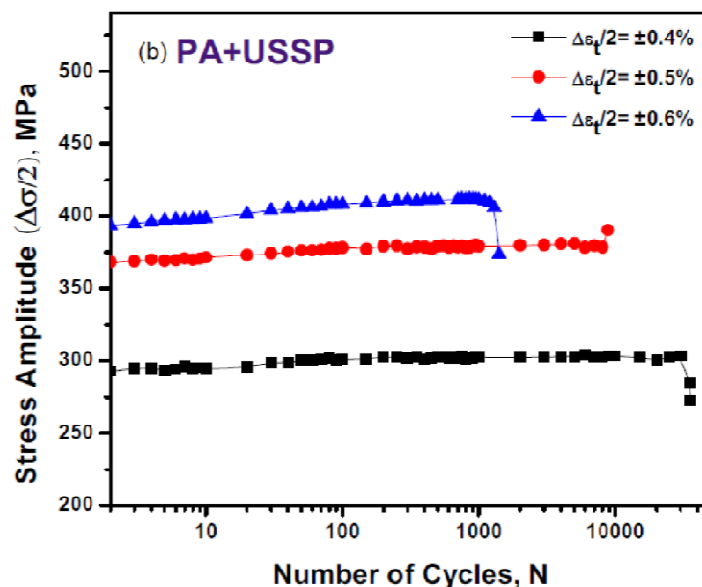
Figure 7 Cyclic stress response curves of the 2014 aluminium alloy at different strain amplitudes: (a) peak aged (b) peak aged & ultrasonic shotpeened.

It may be seen that there was mild cyclic hardening up to 200 cycles both in the peak aged as well as in the peak aged-USSP sample, at all the strain amplitudes and it was followed by near stabilization till failure, except in the case of peak aged condition, in which cyclic hardening was observed before failure.

Fatigue life of the aluminium alloy 2014 in PA and PA+USSP condition at the three strain amplitudes are recorded in Table 4.

Table 4 LCF data of the 2014 aluminium alloy in different conditions

Total strain amplitude, ($\Delta\varepsilon_t/2$)	Fatigue life, N_f (cycles)		Rate of crack propagation (µm/cycle)	
	PA	PA+USSP	PA	PA+USSP
±0.4%	9235	35121	1.34	0.706
±0.5%	4089	8785	2.18	2.05
±0.6%	800	1405	2.43	1.57

It may be seen that there was substantial increase in fatigue life due to shot peening. Fatigue life was increased by 75%, 115% and 280% for the samples tested at strain amplitudes of ±0.6%, ±0.5% and ±0.4% respectively in comparison to that of the un-shotpeened samples. The USSP treatment is seen to be an effective means of enhancing fatigue life of the 2014 aluminium alloy, in particular at the low strain amplitudes. The enhancement in fatigue life due to USSP treatment was found to increase significantly with decrease in strain amplitude.

The dependence of fatigue life on strain amplitude was analyzed using the Coffin–Manson relationship [38] between the plastic strain amplitude ($\Delta\varepsilon_p/2$) and number of reversals to failure ($2N_f$).
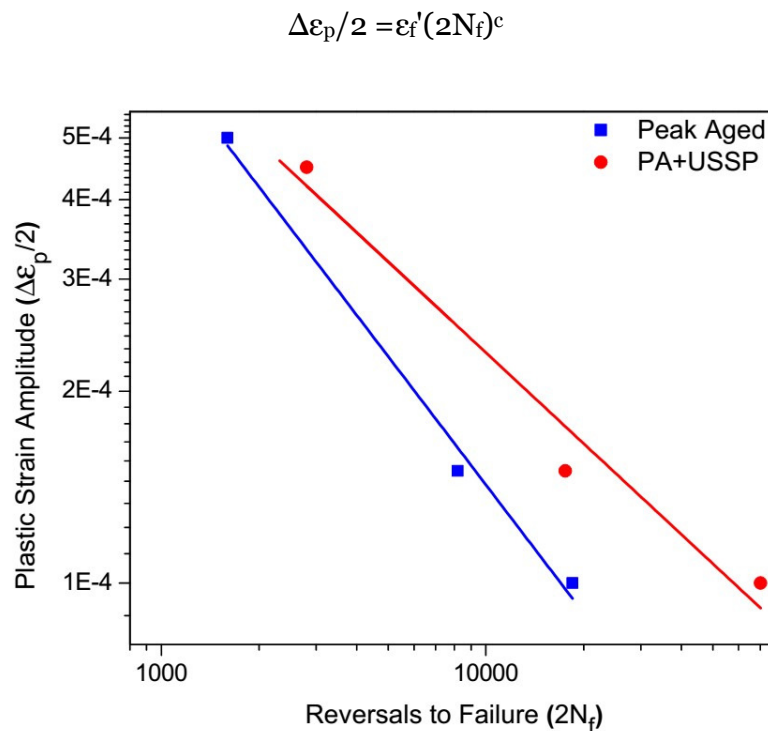
$$\Delta\varepsilon_p/2 = \varepsilon_f'(2N_f)^c$$

Figure 8 Variation of fatigue life with Plastic strain amplitude

Where ε_f' and c are fatigue ductility coefficient and exponent respectively. A linear variation was observed in the plot of $\Delta\varepsilon_p/2$ *vs* $2N_f$ (Fig. 8). It may be seen that fatigue life of the shot peened samples was progressively higher than those of the un-shot peened samples with decrease in strain amplitude.

The cyclic hardening observed during the initial 150 to 200 cycles at all the strain amplitudes, both in the peak aged as well as in peak aged+USSP condition, could be attributed to increase in dislocation density and increasing degree of dislocation-dislocation interaction as well as interactions with the dispersoid particles and strengthening precipitates [42, 43]. This effect was more pronounced at higher strain amplitudes.

Considerable improvement in fatigue life of the shot peened samples was observed at all the strain amplitudes of ±0.40%, ±0.50% and ±0.60%. However, the improvement in fatigue life was highest at the lowest strain amplitude of ±0.4% as compared to that at higher strain amplitudes of ±0.5% and ±0.6%. The increase in fatigue life occurred due to two phenomena,

one from delay in the process of crack initiation because of compressive surface residual stresses which reduced the effective tensile stress and the other was from slower crack growth due to subsurface tensile stresses [29]. Thus, localized plastic deformation in the surface region caused refinement of the microstructure and induced compressive residual stress in the surface layer to resist fatigue crack initiation.

5. Conclusions

Following conclusions may be drawn from the present investigation:

- A layer of nanostructure was formed on the top surface containing nanocrystalline grains of ~30 nm size.
- The USSP process effectively induced surface nanocrystallization in the aluminium alloy 2014.
- Microhardness at the surface increased with peening time and decreased with depth from surface towards interior up to a depth of 500 μm.
- There was no phase transformation due to ultrasonic shot peening.
- Maximum value of tensile stress and yield stress (σ_u and σ_y) for the alloy 2014 was observed in samples peak aged and treated by USSP for 15mins.
- There was significant increase in fatigue life due to USSP. Fatigue life of USSP samples increased progressively with decrease in strain amplitude.

References:

[1] Birringer R, Gleiter H, Klein H, Marquardt P. *Nanocrystalline Materials an Approach to a novel solid structure with gas-like disorder*. Phys Lett A (1984); 102:**365**.

[2] Cahn RW. *Nanostructured materials*. Nature (1990); 348:**389**.

[3] Bohn R, Haubold T, Birringer R, Gleiter H. *Nanocrystalline intermetallic compounds—An approach to ductility*. Scr. Metall. Mater., (1991); 25:**811**.

[4] Koch C. *The Synthesis of Non-Equilibrium Structures by Ball-Milling*. Mater Sci Forum (1992); 243:**88**.

[5] Valiev R, Korznikov A, Mulyukov R. *Structure and properties of ultrafine-grained materials produced by severe plastic deformation*. Mater Sci Eng A (1993); 168:**141**.

[6] Kulik T. *Nanocrystallization of metallic glasses.* Journal of Non-crystalline Solids (2001); 287:**145**.

[7] Erb U, EI-Sherik A, Palumbo G, Aust K. *Synthesis, structure and properties of Electroplated nanocrystalline materials.* Nanostruct. Mater (1993); 2:**383**.

[8] Wu X, Tao N, Hong Y, Xu B, Lu J, Lu K. *Microstructure and evolution of Mechanically - induced ultrafine grain in surface layer of AL-alloy subjected to USSP.* Acta Materialia (2002); 50: **2075–2084.**

[9] Iwahashi Y, Wang Y, Horita J, Nemoto M, Langdon TG. *The Process of Grain Refinement in Equal-Channel Angular Pressing.* Acta mater (1998); 46:**3317**.

[10] Iwahashi Y, Horita Z, Nemoto M, Langdon TG. *An Investigation of Microstructural Evolution during Equal-Channel Angular Pressing.* Acta mater (1997); 45:**4733**.

[11] Shin DH, Kim I, Kim J, Park K. Acta mater (2001); 49:**1285**.

[12] Horita Z, Smith DJ, Nemoto M, Valiev Z, Langdon TG. *Observations of grain boundary structure in submicrometergrained Cu and Ni using high-resolution electron microscopy.* J Mater Res (1998); 13:**446**.

[13] Heilmann P, Clark WAT, Rigney DA. *Orientation determination of subsurface cells generated by sliding.* Acta Metall. (1983); 31:**1293**.

[14] Hughes DA, Dawson DB, Korellis JS, Weingarten LI. *A microstructurally based method for stress estimates.* Wear (1995); 458:**181-183**.

[15] Jang JSC, Koch CC. *The Hall-Petch relationship in nanocrystalline iron produced by ball Milling.* Scripta Metallurgica et Materialia (1990); 24:**1599**.

[16] Fecht HJ, Hellstern E, Fu Z, Johnson WL. *Nanocrystalline Metals Prepared by High-Energy Ball Milling.* Metallurgical and Materials Transactions A (1990); 21:**2333**.

[17] Wang XY, Li DY. *Mechanical and electrochemical behavior of nanocrystalline surface of 304 stainless steel.* Electrochim. Acta. (2002); 47:**3939**.

[18] Wang L, Li DY. Mechanical, Electrochemical and tribological properties of Nanocrystalline surface of brass produced by sandblasting and annealing. Surface and Coating technology (2003); 167:**188**.

[19] Tao NR, Sui ML, Ku J, Lu K. Surface Nanocrystallization of Iron Induced By   Ultrasonic Shot Peening. Nanostructured Mater. (1999); 11:**433**.

[20] Liu G, Lu J, Lu K. Surface nanocrystallization of 316L stainless steel induced by ultrasonic shot peening. Materials Science and Engineering A (2000); 286:**91**.

[21] Liu ZG, Fecht HJ, Umemoto M. Microstructural evolution and nanocrystal formation during deformation of Fe–C alloys. Material science and Engineering A (2004); 839:**375-377**.

[22] Todaka Y, Umemoto M, Tsuchiya K. Comparison of Nanocrystalline Surface Layer in Steels Formed by Air Blast and Ultrasonic Shot Peening. Materials Transactions (2004); 45: **376**.

[23] Guo FA, Trannoy N, Lu J. Analysis of thermal properties by scanning thermal microscopy in nanocrystallized iron surface induced by ultrasonic shot peening. Material Science and Engineering A (2004); 369:**36**.

[24] Wen C, Chen Z, Huang B, Rong Y. Nanocrystallization and Magnetic Properties of Fe-30 Weight Percent Ni Alloy by Surface Mechanical Attrition Treatment. Metallurgical and Materials Transactions (2006); 37A:**1413**.

[22] Umemoto M, Todaka Y, Tsuchiya K. *Formation of Nanocrystalline Structure in Steels by Air Blast Shot Peening*. Mater. Trans (2003); 44:**1488**.

[23] Todaka Y, Umemoto M, Li J, Tsuchiya K. *Nanocrystallization of carbon steels by Shot Peening and Drilling*. Review on Advanced Materials Science (2005); 10:**409**.

[24] Abood AN, Saleh AH, Salem RK, Kadhim GA, Abdullah ZW. *Strain Life of Shot Peening AA 2024-T4*. Journal of Materials Science Research (2013); Vol. 2:No. 1

[25] Curtis S, De los Rios ER, Rodopoulos CA, Levers A .Analysis of the effects of controlled shot peening on fatigue damage of high strength aluminium alloys. International Journal of Fatigue (2003); 25:**59−66**.

[25] Luong H, Hill MR. *The effects of laser peening and shot peening on high cycle fatigue in 7050-T7451 aluminum alloy*. Materials Science and Engineering (2010); A 527:**699−707**.

[26] Cullity BD, *Elements of X-ray Diffraction*, Addison Wesley Publishing, Reading, Massachusetts, 1956.

[31] An Introduction, *Metallography and Microstructures*, Vol 9, ASM Handbook, ASM International, 2004

[32] Singh S, Goel DB. Bull. *Influence of thermomechanical aging on fatigue behaviour of 2014 Al-alloy*. Mater. Sci (April 2005); Vol. 28, No. 2: **91−96**.

[33] Hui-qiong YE, Xin-min FAN. *Surface nanocrystallization of 7A04 aluminium alloy induced by circulation rolling plastic deformation*. Transactions of Nonferrous Metals Society of China (2006); 16:**656-660**.

[34] Roland T, Retraint D, Lu K, Lu J. *Enhanced mechanical behavior of a nanocrystallised stainless steel and its thermal stability*. Materials Science and Engineering A (2007); **445−446:281−288**.

[35] Blonde R, Chan H L, Bonasso N A, Bolle B, Grosdidier T, Lu J. *Evolution of texture and microstructure in pulsed electro-deposited Cu treated by Surface Mechanical Attrition Treatment (SMAT)*. Journal of Alloys and Compounds (2010) **410−413**

[36] Małgorzata W and Jan S. *Recent Trends in Processing and Degradation of Aluminium Alloys*. Intech (2011); p **155-173**.

[37] Chokshi AH, Rosen A, Karch J, Gleiter H. *On the Validity of the Hall-Petch Relationship in Nanocrystalline Materials*. Scr. Metall. (1989); 23:**1119**.

[38] Lu K, Wei WD, Wang JT. *Microhardness and fracture properties of nanocrystalline Ni-P Alloy*. Scr. Metall. Mater. (1990); 24:**2319**.

[39] Dieter GE, *Mechanical Metallurgy*, McGraw-Hill book Company, Singapore, (1988).

[40] Xing YM, Lu K and Lu J. Proceedings of Asian Pacific Conference on Fracture and Strength '01 and International Conference on Advanced Technology in Experimental Mechanics'01 (2001); No 01-203, JSME publisher, Japan, Sendai.

[41] Chen XH, Lu J, Lu L, Lu K. *Tensile properties of a nanocrystalline 316L austenitic stainless steel*. Scripta Materialia (2005); 52:**1039–1044**.

[42] Eswara PN, Malakondaiah G, Kutumbarao VV and Rama RP. Low Cycle Fatigue Behaviour of an Underaged Al-Li-Cu-Mg Alloy. Mater Sci Technol (1996); 12:**563**.

[43] Srivatsan TS, and Coyne EJ, Micromechanisms governing fatigue behaviour of lithium containing aluminium alloys. Mater Sci Technol (1989); 5:**548**.